Drying Technology
An International Journal

ISSN: 0737-3937 (Print) 1532-2300 (Online) Journal homepage: http://www.tandfonline.com/loi/ldrt20

Dehydration, Water Vapor Adsorption and Desorption Behavior of $Zn[B_3O_3(OH)_5] \cdot H_2O$ and $Zn[B_3O_4(OH)_3]$

Burcu Alp , Mehmet Gönen , Sevdiye Atakul Savrık , Devrim Balköse & Semra Ülkü

To cite this article: Burcu Alp , Mehmet Gönen , Sevdiye Atakul Savrık , Devrim Balköse & Semra Ülkü (2012) Dehydration, Water Vapor Adsorption and Desorption Behavior of $Zn[B_3O_3(OH)_5] \cdot H_2O$ and $Zn[B_3O_4(OH)_3]$, Drying Technology, 30:14, 1610-1620, DOI: 10.1080/07373937.2012.701258

To link to this article: http://dx.doi.org/10.1080/07373937.2012.701258

Drying Technology, 30: 1610–1620, 2012

ISSN: 0737-3937 print/1532-2300 online
DOI: 10.1080/07373937.2012.701258

Taylor & Francis
Taylor & Francis Group

Dehydration, Water Vapor Adsorption and Desorption Behavior of $Zn[B_3O_3(OH)_5] \cdot H_2O$ and $Zn[B_3O_4(OH)_3]$

Burcu Alp, Mehmet Gönen, Sevdiye Atakul Savrık, Devrim Balköse, and Semra Ülkü

Chemical Engineering Department, İzmir Institute of Technology, Engineering Faculty, Gülbahçe, Urla, İzmir, Turkey

The dehydration behaviors of two different hydrated zinc borate species, $Zn[B_3O_3(OH)_5] \cdot H_2O$ and $Zn[B_3O_4(OH)_3]$, which are industrially important flame retardants, were studied by thermal gravimetric(TG) analysis and in situ diffuse reflectance infrared Fourier transform (DRIFT) spectroscopy. Dehydration onset temperatures of $Zn[B_3O_3(OH)_5] \cdot H_2O$ and $Zn[B_3O_4(OH)_3]$ were 129 and 320°C, respectively, at a 10°C/min ramp rate. A very small amount of boric acid was volatilized in addition to water vapor when both samples were heated at 250°C. A significant amount of water vapor was adsorbed by $Zn[B_3O_3(OH)_5] \cdot H_2O$ from air at 25°C. However, $Zn[B_3O_4(OH)_3]$ adsorbed a very small amount of water under the same conditions. Both zinc borates did not have a tendency to cake during storage.

Keywords Caking; Dehydration; DRIFT spectroscopy; Water vapor adsorption; Zinc borate

INTRODUCTION

The hydrated borates, which comprise the majority of known boron-containing minerals, and synthetic borates are consumed in various industry branches ranging from insulation, glass, ceramic, detergents, fire retardants, and lubricant additives.[1–3] Hydrated borates are compounds of boron, oxygen, metals, and hydrogen atoms. The basic elements forming the crystalline structure of the borates are trigonal BO_3 and tetrahedral BO_4 groups that form the fundamental building blocks.[4] The composition of borates can be represented by $aM_xO \cdot bB_2O_3 \cdot cH_2O$, where a/c ratio is related to the BO_3:BO_4 ratio of the compound. The value of c represents the degree of condensation of the borate. Zinc borate is an example of a synthetic hydrated metal borate. There are various kinds of crystalline hydrated zinc borates having compositions $4ZnO \cdot B_2O_3 \cdot H_2O$, $ZnO \cdot B_2O_3 \cdot 1 \cdot 12H_2O$, $ZnO \cdot B_2O_3 \cdot 2H_2O$, $6ZnO \cdot 5B_2O_3 \cdot 3H_2O$, $2ZnO \cdot 3B_2O_3 \cdot 7H_2O$, $2ZnO \cdot 3B_2O_3 \cdot 3H_2O$, $3ZnO \cdot 5B_2O_3 \cdot 14H_2O$, and $ZnO \cdot 5B_2O_3 \cdot 4 \cdot 5H_2O$.[5,6] Zinc borate hydrates are formed in water and the type of zinc borate formed changes with temperature, reactant concentration, and pH. $2ZnO \cdot 3B_2O_3 \cdot 7H_2O$ was obtained by addition of zinc oxide to the aqueous solutions of borax and zinc sulfate at the boiling temperature of water, whereas $3ZnO \cdot 5B_2O_3 \cdot 14\ H_2O$ was produced from aqueous mixtures of borax, boric acid, and zinc sulfate.[7] $2ZnO \cdot 3B_2O_3 \cdot 3H_2O$ was transformed to $4ZnO \cdot B_2O_3 \cdot H_2O$ by boiling in boric acid solution.[5] In these products, the B_2O_3:ZnO molar ratio changes from 0.25 to 5 and it plays a significant role in the determination of the structure and characteristics of the product. Therefore, characterization, in particular, determination of dehydration behavior of zinc borate, is of great importance to determine its application area in industry. For instance, zinc borates including a higher number of water molecules in their structure are favored in flame retardant applications in polymers because these kinds of zinc borates can absorb a great amount of heat when their water is released at high temperatures.[8]

The structural formula differentiates the interstitial water and the water present as B-OH in hydrated metal borates.[5,6] For example, industrially important flame retardant zinc borates $3ZnO \cdot 2B_2O_37H_2O$ and $3ZnO \cdot 2B_2O_3 \cdot 3H_2O$ have the structural formulas $Zn[B_3O_3(OH)_5] \cdot H_2O$ and $Zn[B_3O_4(OH)_3]$, respectively.[5,6] $Zn[B_3O_3(OH)_5] \cdot H_2O$ has monomeric triborate dianions in its structure. There are five B-OH groups and one mole of interstitial water in its structural formula. On the other hand, $Zn[B_3O_4(OH)_3]$ is a complex inoborate (containing a borate structural unit that is an infinite chain) composed of linked triborate moieties, interconnected by coordination with pseudo tetrahedral zinc centers and a network of H-bonds.[5] All three OH hydrogens are involved in H-bonding with oxygen atoms of the adjacent chains. They

Present address for Mehmet Gönen: Süleyman Demirel University, Department of Chemical Engineering, Batı Yerleşkesi, Isparta 32260, Turkey.

Present affiliation for Sevdiye Atakul Savrık: AKZO-NOBEL, Izmir, Turkey.

Correspondence: Devrim Balköse, Department of Chemical Engineering, İzmir Institute of Technology, Gülbahçe, Gülbahçe, Urla İzmir 35430, Turkey; E-mail: devrimbalkose@iyte.edu.tr

involve B-O-B acceptor oxygen atoms, not B-O-H oxygens, which explains the high dehydration onset temperature (>290°C) of $Zn[B_3O_4(OH)_3]$. Due to their distinct differences in H-bonding strengths, the three proton sites yield clearly resolved resonances at 4.6, 7.0, and 8 ppm in their nuclear magnetic resonance (NMR) spectra.

Although there are various studies related to the production of zinc borates,[5,8–13] there is not enough information about the dehydration behavior of $Zn[B_3O_3(OH)_5]$. H_2O and $Zn[B_3O_4(OH)_3]$. The dehydration behavior of $Zn[B_3O_4(OH)_3]$ was examined in order to expose its synergistic effect in flame retardancy when used together with $Mg(OH)_2$[14] and to determine its effect on thermal degradation of ammonium polyphosphate.[15] Fourier transform infrared (FTIR) spectroscopy, thermal gravimetric (TG) analysis, and sublimation tests can be used to investigate dehydration behavior. FTIR spectroscopy has been effectively used to identify and characterize solid hydrated borates and their solutions.[16] Characterization of 27 types of hydrated borates was carried out using both FTIR and Raman spectroscopy. Assignments of vibration spectra of monoborates, diborates, triborates, tetraborates, pentaborates, and hexaborates were reported by Jun et al.[17] Moreover, the chemical changes occurring during dry heating of the materials can be determined by in situ FTIR spectroscopy. The change in the intensities of the peaks related to OH groups and H_2O molecules and other functional groups provides information about the changes occurring in the materials. The dehydration behavior of synthetic, natural, and modified zeolites was studied by this technique.[18,19]

TG analysis or continuous mass versus time measurement under controlled atmosphere can be employed to determine the dehydration behaviors of materials as in the cases of $AlF_3 \cdot H_2O$,[20] $Mg(OH)_2$,[21,22] carbamazepine dihydrate,[23] and theralose.[24] The dehydration of chemicals containing free or bound water may lead to the formation of different products. The chemically bound moisture removal from $AlF_3 \cdot 3H_2O$ consisted of two stages. The first is a rapid dehydration stage and the second is a combined dehydration and hydrolysis stage. Hydrolysis causes the formation of undesirable Al_2O_3 and loss of fluorine. Thus, its investigation was essential to elucidate its mechanism in order to minimize undesirable processes.[20] When carbemezine dihydrate was calcined, it transformed into anhydrous form at a rate controlled by the internal diffusion of water to the surface of the crystals,[23] and trehalose dihydrate transformed to an anhydrous β form on drying as well.[24]

Pretreatment of particles before calcination may change the size of the particles. For instance, when $Mg(OH)_2$ was calcined at 550°C it was converted to MgO. The grain diameters of the particles changed in the range of 17–54 nm with different pretreatments before calcination.[22]

TG analysis provides the determination of the onset temperature of dehydration as well as the activation energies of this process. The activation energy values of carbemezine dehydrate were obtained in the range of 61.41–74.56 $kJmol^{-1}$ for agglomerates of particles and plates in isothermal drying experiments at different temperatures.[23]

The formation of nanoparticles of zinc borates by supercritical ethanol drying of zinc borates at 250°C was reported by Dong and Hu.[1] However, extraction of boric acid from zinc borate instead of formation of nanoparticles of zinc borate by supercritical ethanol drying was reported by Gönen et al.[25]

The thermal stability of zinc borates at the temperature used in the supercritical ethanol drying process is important to characterize them in detail. Whether the boric acid was volatilized from the zinc borates by dry heating at the supercritical ethanol extraction temperature could be detected by sublimation tests. During sublimation experiments, water vapor formed is removed from the system by continuous vacuum application. Any condensable vapor such as boric acid is solidified on the cold finger, which is cooled by cold water circulation.

Water vapor adsorption of materials is important in transportation and storage. The adsorbed water may cause the dissolution and recrystallization of materials, which causes sticking of the crystals and caking.[26] Materials that have tendency to adsorb water vapor from the ambient air should be transported and kept in a moisture-free medium to prevent caking, which causes difficulties in handling. If materials were hot during filling and closing of the moisture-proof packages, they continue to dry and a liquid water film forms on the surfaces of crystals, resulting in the crystals sticking to each other by capillary forces during long storage periods.[27] Therefore, the water vapor adsorption and desorption behavior of zinc borates should also be investigated.

In this study, the objective was to determine the dehydration behaviors of $Zn[B_3O_3(OH)_5] \cdot H_2O$ and $Zn[B_3O_4(OH)_3]$ by in situ diffuse reflectance infrared Fourier transform (DRIFT) spectroscopy, TG analysis, and sublimation tests. Furthermore, water vapor adsorption and desorption behaviors of these two zinc borates were examined to understand their tendency toward caking during storage.

METHODS

Two different zinc borates, $Zn[B_3O_3(OH)_5].H_2O$ and $Zn[B_3O_4(OH)_3]$, which were synthesized and characterized in our previous study,[11] were used in the experiments. They were obtained as precipitates from hydrothermal reactions of zinc oxide and boric acid and conventionally dried at 110°C in a hot air oven. TG curves of the samples were obtained using a TGA-51 (Shimadzu, Kyoto, Japan).

Zinc borate samples (10–15 mg) were loaded into an alumina pan and heated from 30 to 600°C at 10°C min^{-1} under N_2 flow (40 mL min^{-1}). For kinetic analysis, samples were also heated at heating rates of 5, 15, and 20°C min^{-1}.

Sublimation experiments for zinc borates and boric acid were performed by heating 1 g of the samples at 250°C under a vacuum using the cold finger setup as shown in Fig. 1a. The samples were heated under a vacuum (at 14.6 kPa pressure) using an oilless vacuum pump (Rocker 300, Today, New Tapei City, Taiwan) on a temperature-controlled hot plate (IKA Rh digital KT/C, IKA Werke, Staufen, Germany) and any sublimed solid matter was condensed on the surface of the cold finger, cooled by water circulation at 25 ± 2°C. During these experiments, the temperature was controlled by measuring the temperature at the junction of the surface of the hot plate and the outside of the glass wall of the heating chamber as shown in Fig. 1a using a thermocouple (0–350°C; ETC1, IKA Werke) and regulating the heat input to the hot plate with the temperature controller (IKA Rh digital KT/C). The temperature at the same point was also monitored using a MiniSight infrared thermometer (Optris, Berlin, Germany) with 1% accuracy.

The FTIR spectra of the samples were collected by an FTS 3000MX (Digilab Excalibur Series, Agilent, Santa Clara, CA, USA) spectrometer at an interval of 4000–400 cm^{-1}. The system was equipped with a DTGS-TEC detector. The DRIFT measurements of dehydration were performed in an in situ heating reaction cell fitted with KBr windows (Harricks, New York). A praying mantis optical geometry (Harricks model) was used to direct the infrared beam. A 0.1-g sample of the zinc borate sample was placed on the sample holder and heated to 500°C at a 2°C min^{-1} heating rate and 0.1 Pa pressure (PT50 vacuum system, Oerlicon Leybold, Cologne, Germany).

Water vapor adsorption isotherms of the samples at 25°C were determined using a temperature- and humidity-controlled chamber (Angelantoni, Cimacolle, Italy). The temperature and relative humidity in the chamber were kept constant ±1°C and ±3%, respectively. The samples were dried at 110°C for 2 h at atmospheric pressure and cooled down to 25°C in a dessicator. They were then placed in Petri dishes on the analytical balance (±0.1 mg accuracy; GP603s, Sartorious AG, Gottingen, Germany) in the chamber and their mass was recorded over time. Because the adsorption was fast and appeared to be completed in the first few minutes of adsorption, the equilibrium data were collected while the humidity increased in steps at 70-min intervals. The chamber had a sealed glove to its left wall to manipulate the sample without opening the system to the atmosphere. The balance in the chamber was observed through a glass window in the door of the chamber. The lids of the Petri dishes were closed until equilibrium constant humidity was obtained during each step change in humidity using the sealed glove attached to the chamber. Data points up to 60% relative humidity were obtained by weighing the sample inside the chamber. The windows of the balance were kept open during the sample equilibration period. They were closed during weighing in order to avoid the air currents present in the chamber. The balance was removed from the chamber and only samples were kept inside after 60% relative humidity. Their weight gain was recorded by covering the lid of the Petri dishes before removal from the chamber. The weighing period (5–10 s) was shorter than the equilibration period of 70 min in the chamber. The adsorbed amounts were similar in duplicate experiments.

The samples dried at 110°C for 2 h were kept in a constant humidity chamber at 75% relative humidity at 25°C for 2 weeks. The dry and water vapor–adsorbed samples were characterized by scanning electron microscopy (SEM; Philips XL 30 SFEG, FEI Company, Hillsboro, OR, USA) for caking and TG analyses were performed by heating at a rate of 10°C min^{-1} to observe water desorption behavior. The moisture-adsorbed samples kept at ambient temperature in sealed containers were checked for caking after 6 months' storage time.

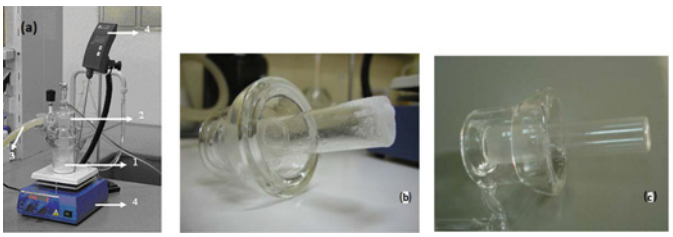

FIG. 1. Photographs of (a) sublimation setup: 1, sublimator; 2, cold finger; 3, vacuum line; 4, temperature-controlled heater; (b) cold finger for pure boric acid; and (c) cold finger for $Zn[B_3O_3(OH)_5] \cdot H_2O$ (color figure available online).

RESULTS AND DISCUSSION

Thermal Gravimetric Analysis

The thermal behavior of zinc borate samples ($Zn[B_3O_3(OH)_5] \cdot H_2O$ and $Zn[B_3O_4(OH)_3]$) is shown in Fig. 2. The upward slope of the TG curves in Fig. 2 during the initial periods of heating was due to a small drift in the baseline of the instrument. The onset temperature for mass loss was accepted as the temperature at which 2% mass loss occurs. The 2% mass loss was observed at 129 and 320°C for $Zn[B_3O_3(OH)_5].H_2O$ and $Zn[B_3O_4(OH)_3]$, respectively. In these TG curves, $Zn[B_3O_3(OH)_5] \cdot H_2O$ and $Zn[B_3O_4(OH)_3]$ show overall mass losses of about 23 and 12%, respectively, in the temperature range of 100 to 450°C under a nitrogen atmosphere. The observed total mass loss in the TG curve of $Zn[B_3O_3(OH)_5] \cdot H_2O$ was consistent with the calculated value of 25.32% water using

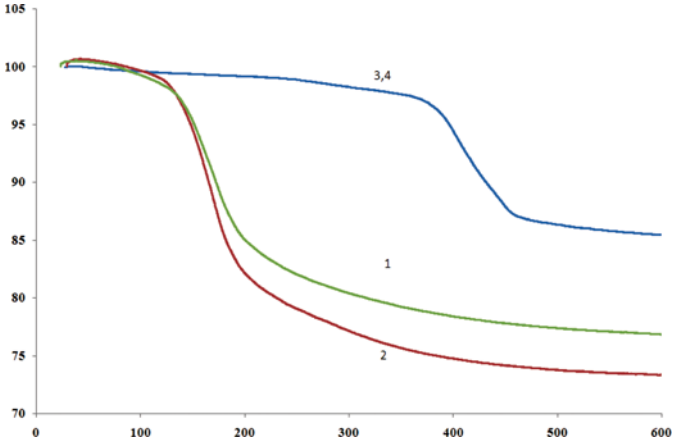

FIG. 2. TG curves of zinc borates: 1, $Zn[B_3O_3(OH)_5] \cdot H_2O$ before water vapor adsorption; 2, $Zn[B_3O_3(OH)_5] \cdot H_2O$ after water vapor adsorption; 3, $Zn[B_3O_4(OH)_3]$ before water vapor adsorption; 4, $Zn[B_3O_4(OH)_3]$ after water vapor adsorption (color figure available online).

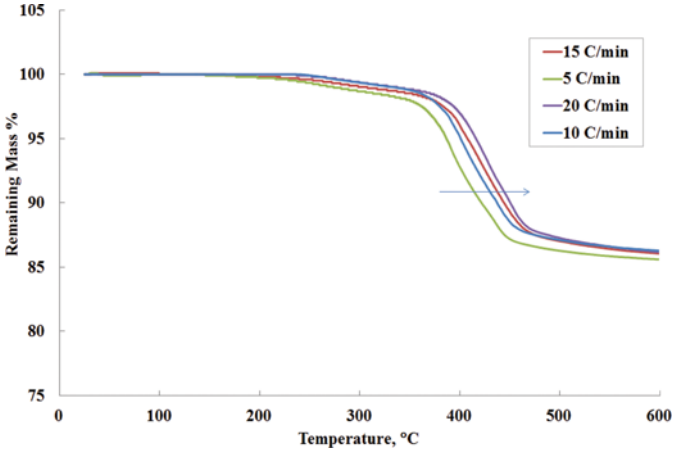

FIG. 3. TG curves of $Zn[B_3O_3(OH)_5].H_2O$ at different heating rates (5, 10, 15, 20°C/min in the direction of the arrow in the figure) (color figure available online).

the chemical formula of zinc borate, $Zn[B_3O_3(OH)_5] \cdot H_2O$. The onset of mass loss of $Zn[B_3O_3(OH)_5] \cdot H_2O$ at 129°C limits its use as a flame retardant additive to polymers that are processed at temperatures lower than this. Zinc borate $Zn[B_3O_4(OH)_3]$ had 12% mass loss, which is comparable to the calculated value of 12.69% for $Zn[B_3O_4(OH)_3]$. $Zn[B_3O_4(OH)_3]$ can be employed as an additive to polymers that are processed at temperatures lower than 320°C. Both $Zn[B_3O_3(OH)_5] \cdot H_2O$ and $Zn[B_3O_4(OH)_3]$ act as flame retardants by releasing water vapor and forming a glassy layer to prevent oxygen diffusion.[5,8,14]

Possible dehydration reactions for two zinc borate samples of $Zn[B_3O_3(OH)_5] \cdot H_2O$ and $Zn[B_3O_4(OH)_3]$ are proposed in Eqs. (1) and (2), respectively:

$$2Zn\left[B_3O_3(OH)_5\right] \cdot H_2O \rightarrow 2ZnO \cdot 3B_2O_3 + 7H_2O \quad (1)$$

$$2Zn\left[B_3O_4(OH)_3\right] \rightarrow 2ZnO \cdot 3B_2O_3 + 3H_2O \quad (2)$$

It was expected that $Zn[B_3O_3(OH)_5] \cdot H_2O$ would provide an amorphous product according to the reaction shown in Eq. (1) when heated. $Zn[B_3O_4(OH)_3]$ dehydrates to yield an amorphous product that corresponds to its dehydrated form according to the reaction shown in Eq. (2).[15] The overall reactions in Eqs. (1) and (2) could occur in several steps. TG curves had only one broad step for both samples, indicating overlapping of individual steps as seen in Fig. 2.

The TG curves obtained by heating the samples at different rates shown in Figs. 3 and 4 were used to determine the activation energy for dehydration of the samples. Ozawa's method[28] was used for this purpose. The activation energy values were calculated by using the slopes of the lines in Figs. 5 and 6, which were obtained by plotting a logarithm of the heating rate versus the inverse of the temperature for different constant extent of dehydration values of the samples and using Eq. (3).

$$\log a = \text{constant} - 0.4567E/RT \quad (3)$$

where a is the heating rate, E is the activation energy, T is the absolute temperature, and R is the gas constant. The lines were linear with regression coefficients of 0.77–0.92 for $Zn[B_3O_3(OH)_5].H_2O$ and 0.87–0.99 for $Zn[B_3O_4(OH)_3]$ as shown in Table 1. The average activation energy values for the drying of $Zn[B_3O_3(OH)_5] \cdot H_2O$ and $Zn[B_3O_4(OH)_3]$ were 54.89 and 166.24 kJ mol^{-1}, respectively, as reported in Table 1. The data range and standard deviation were 96.46 to 78.28% by mass and 5.93 kJ mol^{-1}, respectively, for $Zn[B_3O_3(OH)_5] \cdot H_2O$. The data range and standard

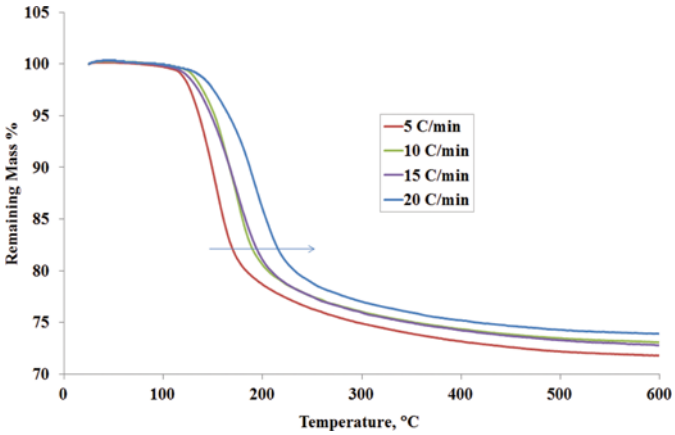

FIG. 4. TG curves of $Zn[B_3O_4(OH)_3]$ at different heating rates (5, 10, 15, 20°C/min in the direction of the arrow in the figure) (color figure available online).

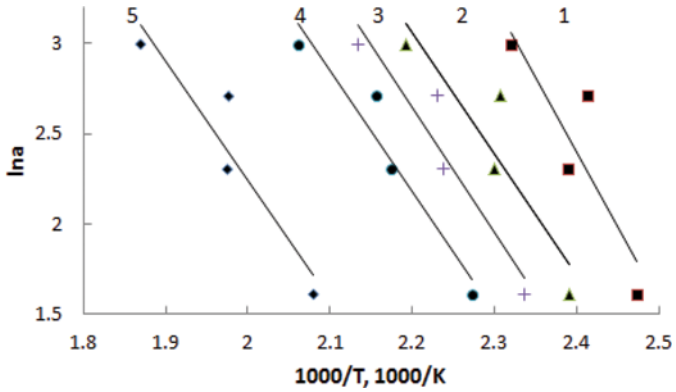

FIG. 5. Ozawa plot[28] of $Zn[B_3O_3(OH)_5] \cdot H_2O$ for 1, 96.46%; 2, 91.92%; 3, 87.37%; 4, 82.83%; 5, 78.28% remaining mass (color figure available online).

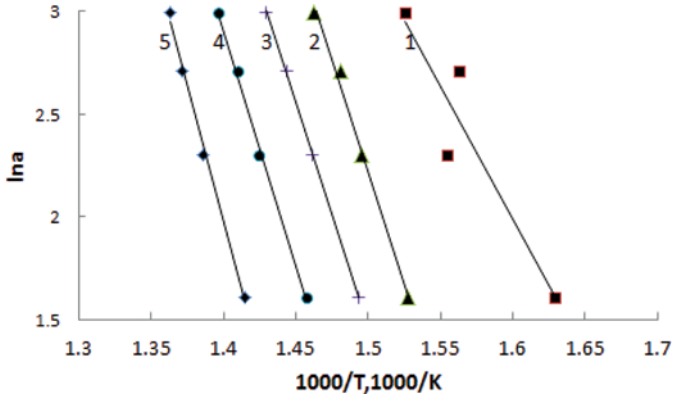

FIG. 6. Ozawa plot[28] for $Zn[B_3O_4(OH)_3]$ for 1, 98.16%; 2, 95.79%; 3, 93.41%; 4, 91.04%; 5, 88.67% remaining mass (color figure available online).

deviation were 98.16 to 88.67% by mass and 12.19 kJ mol^{-1}, respectively, for $Zn[B_3O_4(OH)_3] \cdot Zn[B_3O_4(OH)_3]$ dehydration had higher activation energy than $Zn[B_3O_3(OH)_5]$. H_2O because it involved elimination of water formed by reaction of B-OH groups of inoborate chains as indicated by Eq. (4):

$$\text{B-OH} + \text{B-OH} \rightarrow \text{B-O-B} + H_2O \quad (4)$$

Moisture Desorption

The TG curves of the dry and moist $Zn[B_3O_3(OH)_5]$. H_2O and $Zn[B_3O_4(OH)_3]$ are shown in Fig. 2. Moist samples were kept at 75% relative humidity at 25°C for one week. $Zn[B_3O_3(OH)_5] \cdot H_2O$ adsorbed 3.5% water under these conditions. The mass loss began at 129°C for both dry and moist samples of $Zn[B_3O_3(OH)_5] \cdot H_2O$. The differences in their mass losses were 3 and 3.5% at 180 and 600°C, respectively. Water vapor can be adsorbed physically or chemically. If the water vapor was adsorbed physically, it would be removed up to 110°C. Therefore, TG analysis indicated that the adsorbed water was bound chemically to $Zn[B_3O_3(OH)_5] \cdot H_2O$ because it was desorbed at temperatures higher than 129°C. As seen in Fig. 2, no difference in the TG curves of dried and water vapor–adsorbed samples of $Zn[B_3O_4(OH)_3]$ was observed. This also implied that the amount of water vapor adsorbed by $Zn[B_3O_4(OH)_3]$ was too small to be detected by TG analysis.

Sublimation Test at Supercritical Ethanol Drying Temperature

The decomposition of zinc borates to zinc oxide and boric acid was possible in addition to dehydration during heating of zinc borates. $Zn[B_3O_4(OH)_3]$ was transformed to $4ZnO \cdot B_2O_3 \cdot H_2O$ and boric acid when its aqueous suspensions were heated under reflux conditions.[5] Consequently, the possibility of formation of boric acid should be investigated when pure $Zn[B_3O_4(OH)_3]$ and

TABLE 1
Activation energies of dehydration of $Zn[B_3O_3(OH)_5] \cdot H_2O$ and $Zn[B_3O_4(OH)_3]$

	$Zn[B_3O_3(OH)_5] \cdot H_2O$			$Zn[B_3O_4(OH)_3]$		
	Mass (%)	Regression coefficient	Activation energy (kJ mol^{-1})	Mass (%)	Regression coefficient	Activation energy (kJ mol^{-1})
	96.46	0.77	64.21	98.16	0.87	146.35
	91.92	0.83	55.94	95.79	0.99	170.91
	87.37	0.90	53.82	93.41	0.99	163.46
	82.83	0.92	52.21	91.04	0.99	177.15
	78.28	0.87	48.25	88.67	0.99	173.3
Average			54.89			166.24
Standard deviation			5.93			12.19

$Zn[B_3O_3(OH)_5].H_2O$ are subjected to dry heating. Sublimation tests were performed for this purpose. If boric acid was formed from zinc borate it would be sublimed above 53°C.[29] The sublimation test for boric acid at 250°C resulted in condensation of solid boric acid on the cold finger as seen in Fig. 2b.

Sublimation experiments at the supercritical ethanol drying temperature of 250°C indicated 14.4% mass loss for $Zn[B_3O_3(OH)_5] \cdot H_2O$. TG analysis showed that the mass loss of the product was 16% at 250°C, as seen in Fig. 2. These results are comparable, considering the difference in the accuracy of the temperature control of TG and sublimation experiments. It was not possible to measure the inside temperature of the bottom of the glass chamber of the setup shown in Fig. 1a. The temperature at the outside of the bottom of the glass chamber in Fig. 1a was controlled at 250°C. The temperature monitored by an infrared thermometer was also 250°C at the same point. The actual temperature of the sample inside the bottom of the glass sublimation chamber should have been lower than 250°C due to dissipation of heat to the surroundings. A negligible change in the mass of $Zn[B_3O_4(OH)_3]$ was observed in sublimation tests under the same conditions, confirming the results of TG analysis. However, a very thin solid film of 2–3 mg of mass was formed on the surface of the cold finger as seen in Fig. 2c. The film was scratched with a stainless steel spatula and its FTIR spectrum, shown in Fig. 7, indicated that the film consisted of pure boric acid.[30] Vibrations of boric acid,[30] O-H stretching vibration band at 3230 cm^{-1}, asymmetric stretching vibrations of B-O in the (BO_3) band at 1465 cm^{-1}, a B-O-H in-plane bending vibration band at 1195 cm^{-1}, B-O-H out-of-plane bending vibration at 819 cm^{-1}, deformation vibration of atoms in B-O at 651 cm^{-1}, as well as a B-O-B vibration band at 547 cm^{-1}, were present in the spectrum in Fig. 7.

Only a small amount of boric acid was formed from the initial 1 g of zinc borate samples. This study revealed that heating $Zn[B_3O_3(OH)_5] \cdot H_2O$ at 250°C in the sublimator yielded volatile water vapor as the main product and a very small amount of boric acid.

When zinc borates were heated at 250°C in supercritical ethanol, zinc oxide and boric acid were formed instead of expected nanoparticles of zinc borates.[25] This was not due to the effect of heating but was related to the solvating and extraction of boric acid from zinc borates by ethanol in a supercritical state.

Dehydration Behavior by FTIR Spectroscopy

DRIFT provides information about the processes occurring on the surface of the materials. DRIFT spectra of $Zn[B_3O_3(OH)_5] \cdot H_2O$ and $Zn[B_3O_4(OH)_3]$ under different conditions are exhibited in Figs. 8 and 9, respectively. Spectra from top to bottom in the direction of the arrows represent ambient conditions, after vacuum application at 25°C, and at various temperatures between 125 and 500°C under vacuum. The peaks at 1401 and 1312 cm^{-1} belonged to the vibrations of three coordinate boron (B_3O) groups and peaks at 1192, 1122, 1065, and 1001 cm^{-1} were assigned to the vibrations of four coordinate (B_4O) groups[16,17] and they did not change in intensity during the heating of both samples, as seen in Figs. 8 and 9. The spectra in Figs. 8 and 9 indicate the presence of hydrogen-bonded OH groups and free water on the surfaces of both $Zn[B_3O_3(OH)_5] \cdot H_2O$ and $Zn[B_3O_4(OH)_3]$. The DRIFT spectra of $Zn[B_3O_3(OH)_5] \cdot H_2O$ taken under different conditions are shown in Fig. 8. Though the interstitial water in the structure of $Zn[B_3O_3(OH)_5] \cdot H_2O$ was not affected by vacuum application, it was released from the structure at 125°C as determined by the decrease in the intensity of the band at 1650 cm^{-1} belonging to the vibration of H_2O molecules, as seen in Fig. 8. The

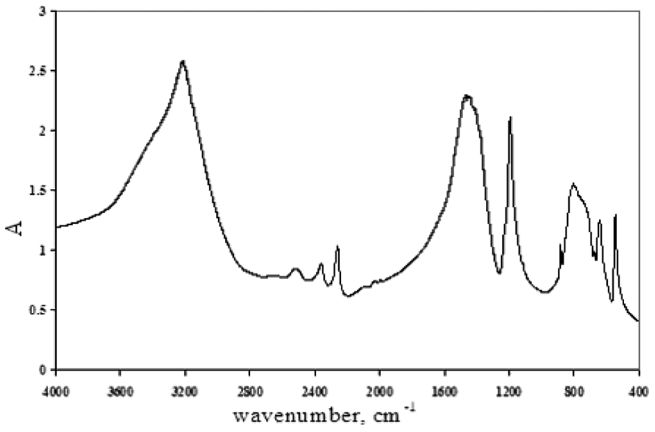

FIG. 7. FTIR spectrum of film formed on cold finger on heating both $Zn[B_3O_3(OH)_5] \cdot H_2O$ and $Zn[B_3O_4(OH)_3]$ at 250°C.

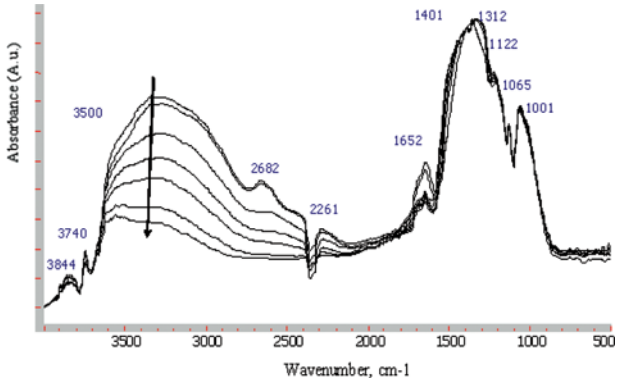

FIG. 8. DRIFT spectra of $Zn[B_3O_3(OH)_5] \cdot H_2O$ in the direction of the arrow: before and after vacuum at room temperature and at different temperatures (125, 205, 300, 400, and 500°C) under vacuum (color figure available online).

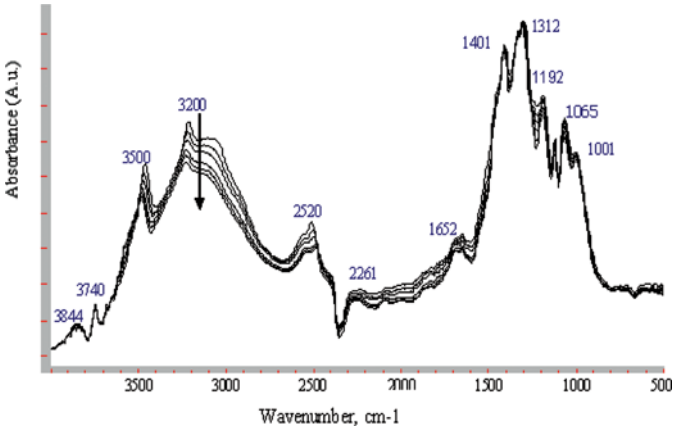

FIG. 9. FTIR spectra of $Zn[B_3O_4(OH)_3]$ in the direction of the arrow direction: before and after vacuum at room temperature and at different temperatures (125, 205, 300, 400, and 500°C) under vacuum (color figure available online).

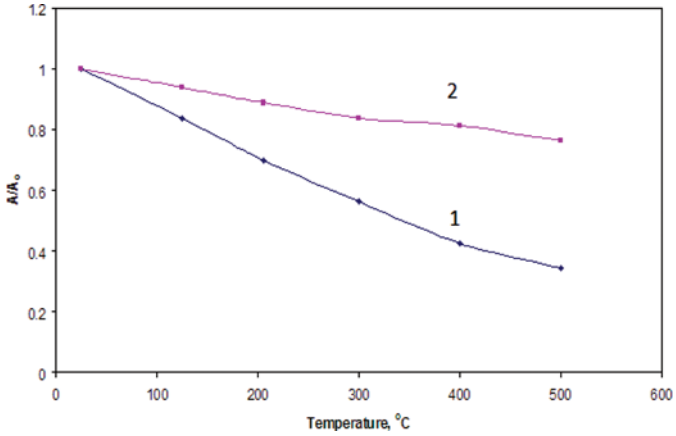

FIG. 10. Change in absorbance ratio (A/A_o) at 3200 cm^{-1} with temperature: 1, $Zn[B_3O_3(OH)_5]\cdot H_2O$; 2, $Zn[B_3O_4(OH)_3]$ (color figure available online).

intensities of the bands at 3400 and 2682 cm^{-1} belonging to O-H groups bound to each other with different hydrogen bond strengths in the structure of $Zn[B_3O_3(OH)_5].H_2O$ decreased with increasing temperature from 125 to 500°C. When $Zn[B_3O_3(OH)_5].H_2O$ is subjected to heating, hydroxyl groups (O-H) create a condensation reaction to form water and zinc borate loses its mass, as exhibited in its TG curve in Fig. 2. DRIFT spectra of zinc borate $Zn[B_3O_4(OH)_3]$ are shown in Fig. 9. The bands at 3500, 3200, and 2520 cm^{-1} could be attributed to OH groups hydrogen-bonded with different strengths with B-O-B oxygens.[5] A small decrease in the absorbance values of these bands at 3500, 3200, and 2520 cm^{-1} belonging to O-H groups in the structure of $Zn[B_3O_4(OH)_3]$ was observed during the increase of the temperature.

The absorbance values (A) at 3200 cm^{-1} in the FTIR spectra of $Zn[B_3O_3(OH)_5]\cdot H_2O$ and $Zn[B_3O_4(OH)_3]$ heated to different temperatures were measured. The absorbance value at 25°C was taken as a reference (A_o) and the variation in the ratio (A/A_o) with respect to temperature is shown in Fig. 10. It could be proposed that zinc borate $Zn[B_3O_4(OH)_3]$ was not influenced greatly with rising temperature, because the change in absorbance ratio between 25 and 500°C was only 22%. On the other hand, $Zn[B_3O_3(OH)_5]\cdot H_2O$ was substantially affected by increasing temperature because the change in the absorbance ratio for the same temperature range was 72%. Dehydration of both zinc borate samples was not complete at 500°C, as indicated by the presence of hydrogen-bonded OH group vibrations. Further heating at higher temperatures is required to obtain anhydrous crystals.

The absorbance values (A) of the peak at 1650 cm^{-1} that belonged to H_2O bending vibration in the FTIR spectra of $Zn[B_3O_3(OH)_5]\cdot H_2O$ and $Zn[B_3O_4(OH)_3]$ heated to different temperatures were measured. The absorbance value at 25°C was taken as a reference (A_o) and the variation in the ratio (A/A_o) at 1650 cm^{-1} with respect to temperature is shown in Fig. 11. The absorbance ratio values were decreased to lower values at lower temperatures at 1650 cm^{-1} than at 3200 cm^{-1} for both $Zn[B_3O_3(OH)_5]\cdot H_2O$ and $Zn[B_3O_4(OH)_3]$. The absorbance ratios at 1650 cm^{-1} decreased to 0.86 and 0.50 for $Zn[B_3O_4(OH)_3]$ and $Zn[B_3O_3(OH)_5]\cdot H_2O$, respectively, at 200°C. The absorbance ratios observed for hydrogen-bonded OH groups peak at 3200 cm^{-1} were 0.88 and 0.69 for $Zn[B_3O_4(OH)_3]$ and $Zn[B_3O_3(OH)_5]\cdot H_2O$, respectively, at the same temperature. However, at 500°C, absorbance ratios of 0.60 and 0.35 at 1650 cm^{-1} were observed for $Zn[B_3O_4(OH)_3]$ and $Zn[B_3O_3(OH)_5]\cdot H_2O$, respectively. The absorbance ratios at 3200 cm^{-1} at the same temperature were 0.78 and 0.38 for $Zn[B_3O_4(OH)_3]$ and $Zn[B_3O_3(OH)_5]\cdot H_2O$, respectively. This showed that the water already present

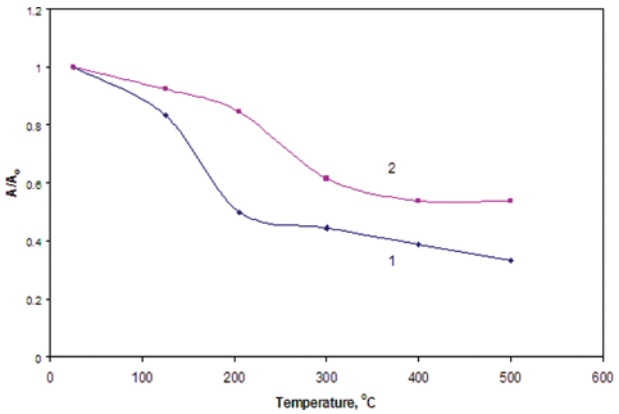

FIG. 11. Change in absorbance ratio (A/A_o) at 1650 cm^{-1} with temperature: 1, $Zn[B_3O_3(OH)_5]\cdot H_2O$; 2, $Zn[B_3O_4(OH)_3]$ (color figure available online).

in the samples was removed at lower temperatures than hydrogen-bonded OH groups from both samples.

The change in absorbance ratio with temperature at 3060 cm^{-1} for $Zn[B_3O_3(OH)_5].H_2O$ and at 2680 cm^{-1} for $Zn[B_3O_4(OH)_3]$ shown in Fig. 12, curves 1 and 2, respectively, demonstrated greater removal of hydrogen-bonded OH groups in $Zn[B_3O_3(OH)_5].H_2O$.

Though DRIFT data show the changes in concentration of functional groups on the surface, TG shows mass transfer from the bulk solid to vapor. Though FTIR images show a continuous decrease of O-H groups of the samples in Figs. 10–12, the TG curves in Fig. 2 indicate step changes in the mass at 129 and 320°C for $Zn[B_3O_3(OH)_5] \cdot H_2O$ and $Zn[B_3O_4(OH)_3]$ due to evaporation of H_2O present in the samples or formed by the reaction of OH groups with increasing temperature. FTIR spectroscopy indicated that H_2O was originally present in the samples and water of crystallization were removed at lower temperatures than the H_2O formed by the reaction of bound OH groups with each other as represented by Eq. (4). At 500°C both samples were not in anhydrous form they had still OH groups in their structure, as determined by their FTIR spectra.

Moisture Adsorption Kinetics

The rate of adsorption on zinc borates was very fast, as seen in Fig. 13, for selected relative humidity values at 25°C. Adsorption was nearly complete in the first few minutes and equilibrium appeared to be established in this period. In Fig. 13 the moisture content of the sample changed as the step increase in relative humidity was realized. For example, when the relative humidity was increased from 10 to 20% the solid moisture changed from 3.8 to 5.8% immediately, as seen in Fig. 14. Adsorption occurred on the surface and water did not diffuse to the inside of the nonporous particles.

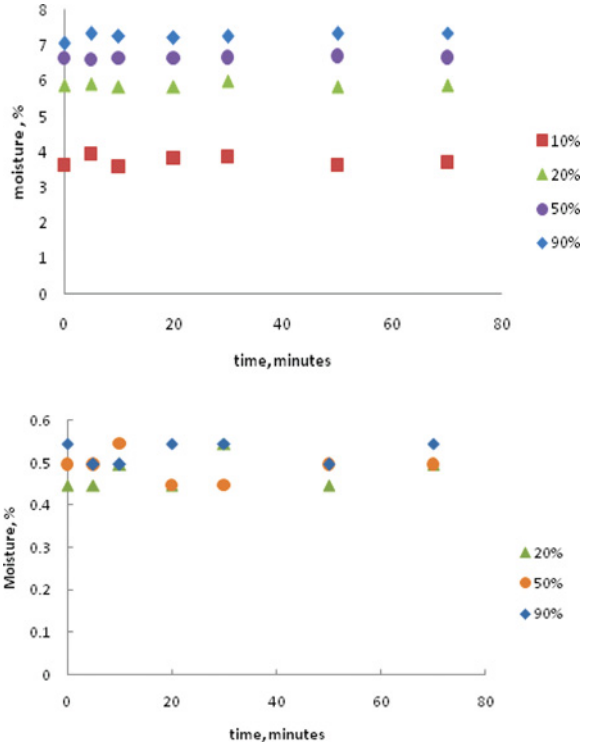

FIG. 13. Change in the percentage moisture content of the samples with time at different relative humidity values at 25°C for (a) $Zn[B_3O_3(OH)_5] \cdot H_2O$ and (b) $Zn[B_3O_4(OH)_3]$ (color figure available online).

Moisture Adsorption Isotherms

Moisture adsorption isotherm of solids can be determined using saturated salt solutions to obtain constant water activities (humidity, %).[31,32] The samples kept in atmospheres with different water activities were weighed against time until their mass was unchanged. However, the mass of samples that were taken out of the controlled atmospheres to ambient air for weighing could change during this transfer process. There are more automated

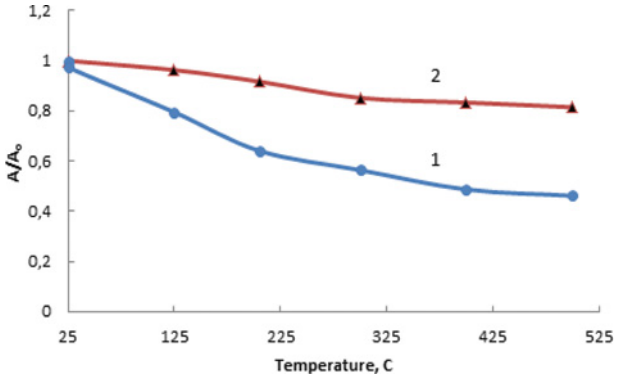

FIG. 12. Change in absorbance ratio (A/A_o) with temperature: 1, at 3060 cm^{-1} for $Zn[B_3O_3(OH)_5] \cdot H_2O$; 2, at 2680 cm^{-1} for $Zn[B_3O_4(OH)_3]$ (color figure available online).

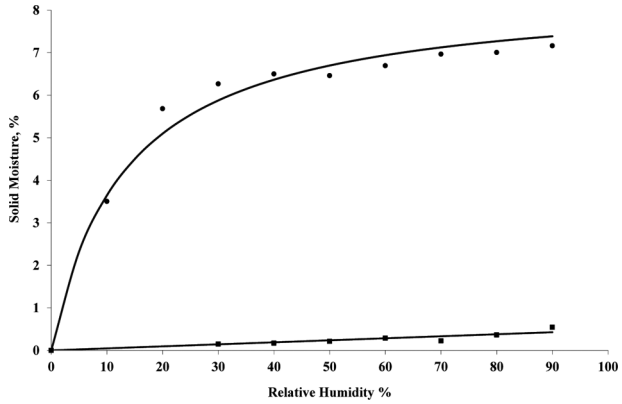

FIG. 14. Adsorption isotherm of water vapor on 1, $Zn[B_3O_3(OH)_5].H_2O$ (dots); 2, $Zn[B_3O_4(OH)_3]$ (squares); lines represent models in Eqs. (5) and (6).

techniques of which the sample was not transferred for weighing. In the present study, the samples were kept in a humidity chamber for a 70-min equilibrium time period. Weighing of the samples up to 60% relative humidity at 25°C was done using a balance with 0.1 mg sensitivity that was placed in the climatic chamber. At higher relative humidity values the balance was taken outside the chamber for protection from moisture. Dynamic vapor sorption[23] and gravimetric sorption techniques[33] are more appropriate methods for the study of the thermodynamic and adsorption–desorption kinetics of samples in controlled atmosphere. The water vapor adsorption isotherms of $Zn[B_3O_4(OH)_3]$ and $Zn[B_3O_3(OH)_5]\cdot H_2O$ at 25°C are shown in Fig. 14. The adsorption data for $Zn[B_3O_4(OH)_3]$ were fitted to a linear isotherm with a regression coefficient of 0.85 and the data for $Zn[B_3O_3(OH)_5]\cdot H_2O$ were fitted to Langmuir adsorption isotherm with a regression coefficient of 0.95 as represented by Eqs. (5) and (6), respectively:

$$q = 0.0047a_w \tag{5}$$

$$q = 0.63a_w/(1 + 0.075a_w) \tag{6}$$

where q is the moisture content of solids (mass %) and a_w is the activity of water vapor in air as a percentage of relative humidity at 25°C. Though $Zn[B_3O_4(OH)_3]$ adsorbed a very small amount of moisture from the ambient air, $Zn[B_3O_3(OH)_5]\cdot H_2O$ adsorbed up to 6–7% moisture at high relative humidity values. TG analysis of the moisture adsorbed samples indicated that the water vapor was chemically adsorbed to $Zn[B_3O_3(OH)_5]\cdot H_2O$.

Tendency of Caking of Zinc Borates during Storage

Two types of zinc borates were tested to determine whether they cake during storage in humid atmospheres. Both zinc borates were nearly insoluble in liquid water. Thus, the caking behavior due to dissolution in water and reprecipitation at the surface of water-soluble substances such as boric acid[26] and ammonium nitrate[27] was not expected. The caking characteristics of $Zn[B_3O_3(OH)_5]\cdot H_2O$ in a dry state and after aging at 75% relative humidity at 25°C for 2 weeks were examined by SEM. The crystals were in lamellar shapes with an average length of 2 μm, width of 0.5 μm, and thickness of 100 nm. In Fig. 15a the micrograph of the dry particles at 1,000× magnification shows that the particles were agglomerated to granules of 20 μm in size. The arrow in the figure indicates an agglomerated granule. $Zn[B_3O_3(OH)_5]\cdot H_2O$ was obtained by drying the crystals formed in aqueous solutions. The surface tension of the water during the drying process caused agglomeration of the particles.[27] The micrographs of $Zn[B_3O_3(OH)_5]\cdot H_2O$ at 5,000× in Fig. 15c and 10,000× in Fig. 15e also indicated that the particles were agglomerated. The particles packed to a smaller volume but there was no evidence of sticking after moisture adsorption, as seen in Figs. 15b, 15d, and 15f. The adsorbed moisture did not cause dissolution, recrystallization, and sticking of the particles. Water adsorbed was bound chemically to $Zn[B_3O_3(OH)_5]\cdot H_2O$; the original agglomerates obtained by conventional drying were broken and the particles packed closer in space in water-adsorbed state. The arrow in the figure indicates better packing of the particles. SEM micrographs of $Zn[B_3O_4(OH)_3]$ can been seen in Figs. 16a and 16b at 2,500× and 20,000× magnification, respectively. The crystals were 1 μm in a dry state. $Zn[B_3O_4(OH)_3]$ adsorbed a very small amount of moisture and no change was observed in its appearance

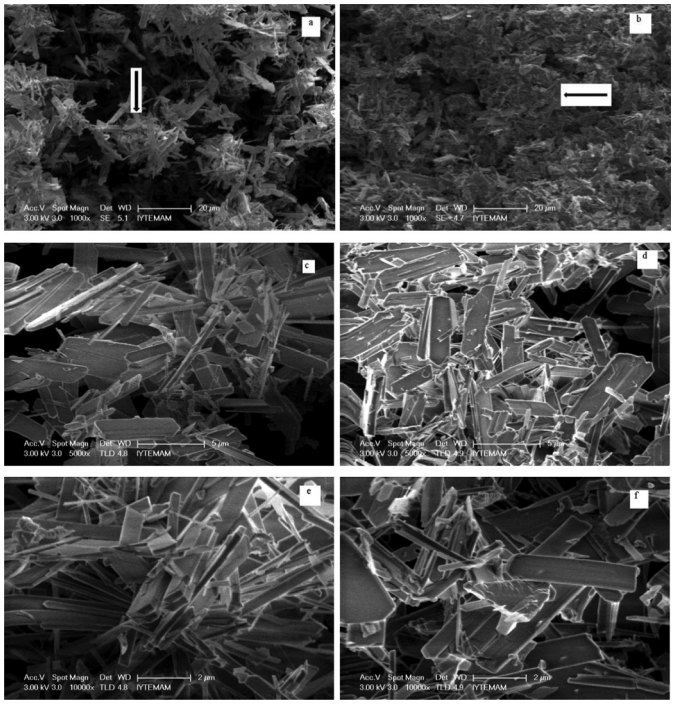

FIG. 15. SEM micrographs of $Zn[B_3O_3(OH)_5]\cdot H_2O$ at different magnifications: (a) dried state at 1,000× (arrow indicates an agglomerate of particles); (b) after storage at 75% relative humidity at 25°C at 1,000× (arrow indicates better packed particles); (c) dried state at 5,000×; (d) after storage at 75% relative humidity at 25°C at 5,000×; (e) dried state at 10,000×; (f) after storage at 75% relative humidity at 25°C at 10,000×.

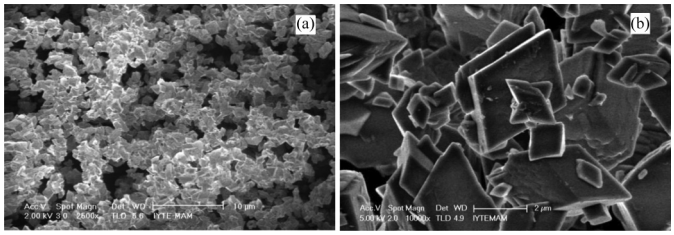

FIG. 16. SEM micrograph of $Zn[B_3O_4(OH)_3]$ at different magnifications: (a) 2,500× and (b) 20,000×.

when stored in a humid atmosphere. Both $Zn[B_3O_3(OH)_5] \cdot H_2O$ and $Zn[B_3O_4(OH)_3]$ did not cake and their powder flowed freely after 6 months' storage in a water-adsorbed state at ambient temperature in sealed containers.

CONCLUSION

This study shows the thermal and dehydration behavior of synthesized zinc borates. Two different zinc borates, $Zn[B_3O_3(OH)_5] \cdot H_2O$ and $Zn[B_3O_4(OH)_3]$, were obtained from zinc oxide and excess boric acid in aqueous media at 60°C and further heating at 90°C, respectively. $Zn[B_3O_3(OH)_5] \cdot H_2O$ and $Zn[B_3O_4(OH)_3]$ dehydrated with 24 and 12% mass losses due to evaporation of the water initially present and formed by the condensation of B-OH groups mainly at around 129 and 320°C, respectively. Parallel to dehydration, a negligible amount of boric acid was sublimed from both zinc borates on heating up to 250°C. FTIR showed decreased intensities of the peaks for the hydrogen-bonded OH groups at 3200 cm^{-1} and the bending vibration of water at 1650 cm^{-1}. Analysis using Ozawa's method showed lower average activation energy values for the drying of $Zn[B_3O_3(OH)_5] \cdot H_2O$ than $Zn[B_3O_4(OH)_3]$. Though $Zn[B_3O_3(OH)_5] \cdot H_2O$ adsorbed water vapor from the air at 90% relative humidity, only a very small amount of water was adsorbed by $Zn[B_3O_4(OH)_3]$ under the same conditions. TG analysis indicated that adsorbed water was bound chemically to $Zn[B_3O_3(OH)_5] \cdot H_2O$. No caking was observed for both types of zinc borates after 6 months' storage time at ambient temperature in a water vapor–adsorbed state in closed containers. However, $Zn[B_3O_3(OH)_5].H_2O$ should be stored in a dry atmosphere in order to prevent its transformation into other products.

ACKNOWLEDGMENTS

This study was supported by TÜBİTAK project number 105M358. The authors thank Dr. Allahverdiev for his contribution to the experimental study.

REFERENCES

1. Dong, J.X.; Hu, Z.S. A study of the anti-wear and friction-reducing properties of the lubricant additive, nanometer zinc borate. *Tribology International* **1998**, *31*, 219–223.
2. Hu, Z.S.; Dong, J.X.; Chen, G.X.; Lou, F. Preparation of nanometer copper borate with supercritical carbon dioxide drying. *Powder Technology* **1999**, *102*, 171–176.
3. Savrık, S.A.; Balkose, D.; Ulku, S. Synthesis of zinc borate by inverse emulsion technique for lubrication. *Thermal Analysis and Calorimetry* **2011**, *104*, 605–612.
4. Waclawska, I. Controlled rate thermal analysis of hydrated borates. *Journal of Thermal Analysis* **1998**, *53*, 519–532.
5. Schubert, D.M.; Alam, F.; Visi, M.Z.; Knobler, C.B. Structural characterization and chemistry of industrially important zinc borate $Zn[B_3O_4(OH)_3]$. *Chemistry of Materials* **2003**, *15*, 866–871.
6. Schubert, D.M. Borates in industrial use. In *Group 13 Chemistry III Industrial Applications*; Roesky, H.W.; Atwood, D.A., Eds.; Springer: Berlin, 2003; 1–40.
7. Gao, Y.H.; Liu, Z.H. Synthesis and thermochemistry of two zinc borates, $Zn_2B_6O_{11}.7H_2O$ and $Zn_3B_{10}O_{18}.14H_2O$. *Thermochimica Acta* **2009**, *484*, 27–31.
8. Schubert, D.M. Zinc Borate. U.S. Patent No. 5472644, 1995.
9. Nies, N.P.; Hulbert, R.W. Zinc Borate of Low Hydration and Method for Preparing the Same. U.S. Patent No. 3549316, 1970.
10. Sawada, H.; Igarashi, H.; Sakao, K. Zinc Borate and Production Method and Use Thereof. U.S. Patent No. 6780913 B2, 2004.
11. Shete, A.V.; Sawant, S.B.; Pangarkar, V.G. Kinetics of fluid–solid reaction with an insoluble product: Zinc borate by the reaction of boric acid and zinc oxide. *Journal of Chemical Technology and Biotechnology* **2004**, *79*, 526–532.
12. Eltepe, H.E.; Balköse, D.; Ülkü, S. Effect of temperature and time on zinc borate species formed from zinc oxide and boric acid in aqueous medium. *Industrial and Engineering Chemistry Research* **2007**, *46*, 2367–2371.
13. Gürhan, D.; Çakal, G.Ö.; Eroğlu, İ.; Özkar, S. Improved synthesis of fine zinc borate particles using seed crystal. *Journal of Crystal Growth* **2009**, *311*, 1545–1552.
14. Genovese, A.; Shanks, R.A. Structural and thermal interpretation of the synergy and interactions between fire retardents magnesium hydroxide and zinc borate. *Polymer Degradation and Stability* **2007**, *92*, 2–13.
15. Samyn, F.; Bourbigot, S.; Duquesne, S.; Delobel, R. Effect of zinc borate on the thermal degradation of ammonium polyphosphate. *Thermochimica Acta* **2007**, *456*, 134–144.
16. Zhihong, L.; Bo, G.; Mancheng, H.; Shuni, L.; Shuping, X. FT-IR and Raman spectroscopic analysis of hydrated cesium borates and their saturated aqueous solution. *Specrochimica Acta Part A* **2003**, *59*, 2741–2745.
17. Jun, L.; Shupping, X.; Shiyang, G. FT-IR and Raman spectroscopic study of hydrated borates. *Spectrochimica Acta Part A: Molecular and Biomolecular Spectroscopy* **1995**, *51*(4), 519–532.
18. Beta, I.A.; Èhlig, H.B.; Hunger, B. Investigation of the non-isothermal water desorption on alkali–metal cation-exchanged X-type zeolites: A temperature-programmed diffuse reflection infrared Fourier transform spectroscopic (TP-DRIFTS) study. *Thermochimica Acta* **2000**, *361*, 61–68.
19. Narin, G.; Balköse, D.; Ulku, S. Characterization and dehydration behavior of a natural, ammonium hydroxide, and thermally treated zeolitic tuff. *Drying Technology* **2011**, *29*, 554–565.
20. Yang, G.Y.; Shi, Y.C.; Liu, X.D.; Mujumdar, A.S. TG-DTG analysis of chemically bound moisture removal of $AlF_3 \cdot 3H_2O$. *Drying Technology* **2007**, *25*, 675–680.
21. Yun, L.; Wang, B.; Jing, D.; Lv, X.; Yu, C.; Wang, G.; Huang, L.; Mujumdar, A.S. Drying kinetics of magnesium hydroxide of different morphological micro nano structures. *Drying Technology* **2010**, *27*, 523–528.
22. Wang, B.H.; Zhang, W.B.; Zhang, W.; Yu, C.Y.; Wang, G.; Huang, L.X.; Mujumdar, A.S. Influence of drying processes on agglomeration and grain diameters of magnesium oxide nanoparticles. *Drying Technology* **2007**, *25*, 715–721.
23. Khoo, J.Y.; Williams, D.R.; Heng, J.Y.Y. Dehydration kinetics of pharmaceutical hydrate: Effects of environmental conditions and crystal forms. *Drying Technology* **2010**, *28*, 1164–1169.
24. Ohashi, T.; Yoshii, H.; Furuta, T. Effect of drying methods on crystal transformation of trehalose. *Drying Technology* **2007**, *25*, 1305–1311.
25. Gönen, M.; Balköse, D.; Ülkü, S. Supercritical ethanol drying of zinc borates of $2ZnO \cdot 3B_2O_3 \cdot 3H_2O$ and $ZnO \cdot B_2O_3 \cdot 2H_2O$. *The Journal of Supercritical Fluids* **2011**, *59*, 43–52.

26. Cleaver, J.A.S.; Cleaver, K.G.; Louis, S.; Hayati, I. Moisture induced caking of boric acid. *Powder Technology* **2004**, *146*, 93–101.
27. Walker, G.M.; Magee, T.R.A.; Holland, C.R.; Ahmad, M.N.; Fox, J.N.; Kells, A.G. Granular fertilizer drying and agglomeration in storage. *Drying Technology* **2000**, *18*, 493–502.
28. Ozawa, T. A new method of analyzing thermogravimetric data. *Bulletin of the Chemical Society of Japan* **1965**, *38*, 1881–1886.
29. Pankajavalli, R.; Anthonysmy, S.; Anahtasivan, K.; Rao, P.R.V. Vapour pressure and enthalpy of sublimation of H_3BO_3. *Journal of Nuclear Materials* **2007**, *362*, 128–131.
30. Medvedev, E.F.; Komarevskaya, S. IR spectroscopic study of the phase composition of boric acid as a component of glass batch. *Glass and Ceramics* **2007**, *64*, 42–46.
31. Abdulla, G.; Belghit, A.; Allaf, K. Impact of instant controlled pressure drop treatment on moisture adsorption isotherm of cork granules. *Drying Technology* **2009**, *27*, 237–247.
32. Gilbert, O.; Meot, J.M.; Marouze, C.; Brouat, J. Low cost device for constructing sorption isotherms. *Drying Technology* **2006**, *24*, 1697–1704.
33. Karoglou, M.; Moropoulou, A.; Maroulis, Z.B.; Krokida, M.K. Water sorption isotherms of some building materials. *Drying Technology* **2005**, *23*, 289–303.